Journal of Molecular Liquids 366 (2022) 120144

Contents lists available at ScienceDirect

Journal of Molecular Liquids

journal homepage: www.elsevier.com/locate/molliq

# Structure and electronic characterization of pristine and functionalized single wall carbon nanotube interacting with sulfide ion: A density functional theory approach

Sania Bibi [a], Sehrish Sarfaraz [b], Muhammad Yar [b], Muhammad Iqbal Zaman [a,*], Abdul Niaz [a], Ayesha Khan [c], Muhammad Ali Hashmi [d], Khurshid Ayub [b,*]

[a] Department of Chemistry, University of Science & Technology Bannu, 28100 Bannu, KP, Pakistan
[b] Department of Chemistry, COMSATS University, Abbottabad Campus, KP 22060, Pakistan
[c] School of Chemical and Physical Sciences, Victoria University of Wellington, Wellington 6012, New Zealand
[d] Department of Chemistry, Division of Science & Technology, University of Education, 54770 Lahore, Pakistan

ARTICLE INFO

*Article history:*
Received 16 May 2022
Revised 15 August 2022
Accepted 18 August 2022
Available online 24 August 2022

*Keywords:*
Density functional theory
Single wall carbon nanotube
Sulfide ion
Charge analysis
HOMO-LUMO energies

ABSTRACT

Density functional theory (DFT) and Time Dependent Density functional theory (TD-DFT) calculations were performed to study the interaction of sulfide ion with pristine and edge/sidewall covalently functionalized single wall carbon nanotube (SWCNT, OH+$NH_2$-SWCNT and COOH+$NH_2$-SWCNT). NBO and Mulliken charge transfer between sulfide ion and pristine, edge/sidewall functionalized SWCNT (OH +$NH_2$-SWCNT and COOH+$NH_2$-SWCNT) was analyzed and a greater effect of charge transfer from analyte (sulfide ion) to SWCNT was calculated for sidewall functionalized carbon nanotube (COOH+$NH_2$-SWCNT-$S^{2-}$). Further, the electronic properties like ionization potential (IPs), electron affinities (EAs), and frontier molecular orbitals analysis were computed. Upon interaction appreciable decrease in energy gap is observed in all studied systems, however, the least energy gap is obtained in case of sidewall functionalized COOH+$NH_2$-SWCNT-$S^{2-}$. The simulated vibrational frequencies of both pristine and functionalized SWCNT interacting with sulfide ion were in good correlations with the reported literature. Similarly, the UV–Vis–NIR spectral bands for SWCNT-$S^{2-}$, OH+$NH_2$-SWCNT-$S^{2-}$ and COOH+$NH_2$-SWCNT-$S^{2-}$ have been analyzed at TD-DFT-ωB97XD/6-31G (d,p). DFT study has revealed that the sidewall functionalized COOH+$NH_2$-SWCNT has a greater sensing ability towards sulfide ion over the pristine SWCNT.



## 1. Introduction

Carbon nanotubes (CNTs), since their discovery in 1991 [1], have gained a great attention in material sciences [2] due to their unique chemical, mechanical, elastic properties [3,4] and high thermal stability [5]. Further, CNTs are highly appreciated for their higher conductivities [6,7] and unique electronic properties [8] which make them the promising candidates for applications in various fields of sciences [9]. However, there are certain limitations with the use of pristine CNTs due to their inert nature. For instance, CNTs have high van der Waals forces between tubes which give them high cohesive energy and are therefore insoluble in water and in some common solvents [10]. Such properties restrict the chemical approaches and synthesis of composite materials at nano scale. Therefore, to make them useful, several methods are available in the literature to modify the properties of CNTs. For this purpose, chemical functionalization of CNTs is an attractive approach to improve their solubility and processibility [11,12]. By using this approach, the cohesive energies in CNTs are reduced and they become soluble. The important step in the functionalization is the oxidation of CNTs walls by some important functional groups such as COOH [13,14], OH [15], $NH_2$ [16], halogens [17,18] and various complexes [19,20]. These groups are attached either at the edge or at the side walls of the CNTs. Mostly, SWCNTs are functionalized due to their simple structural and mono-molecular characteristics which make them interesting and easier to handle for chemical functionalization. Such functionalized CNTs are finest materials used in chemical and biological applications [21,22] particularly for the sensing and monitoring of gases [23], heavy metals [24] and other toxic ions [25].

Like various compounds, anions of sulfur in the form of sulfide have several applications as a byproduct in different industries

* Corresponding authors.
*E-mail addresses:* mizaman@ustb.edu.pk (M.I. Zaman), khurshid@cuiatd.edu.pk (K. Ayub).

https://doi.org/10.1016/j.molliq.2022.120144
0167-7322/

[26]. It is originated from the reduction of sulfates and from the decompositions of organic compounds. However, despite its uses in various applications, sulfide ion causes serious problems to human health which are mostly respiratory issues and mucous membrane toxicity [27]. Therefore, it is important to develop methods which can detect sulfide ion in water bodies. For this purpose, various experimental technologies such as spectroscopic techniques [28,29], chromatographic analysis [30] and electrochemical methods [31] have been applied for the adsorption and detection of sulfide from the various effluents. Although these available techniques are sensitive and robust but, they have limitation in on point and detection. Beside these inherent shortcomings these techniques required sophisticated and expensive instruments, and complex sample preprocesses [32]. Large number of gas molecules, for example $SO_2$, $H_2S$ and $SO_2F_2$ etc., can adsorb on the CNTs surface by means of chemical or physical interactions, thus led to the redistribution of the electronic structure. Upon adsorption, these gases bring perturbation in the conductivity of CNTs, therefore, making them suitable candidates in sensing applications [33]. Goyenola, et al. demonstrated through DFT calculations that the pure hexagonal networks exhibit higher stability as compared to defects containing graphene as long as the sulfur content is up to 10 at. % [34,35]. Lin et al.[36] have studied the effect of adsorption of $NH_3$ and $CO_2$ on Ag decoration of CNTs. Their results reveal that Ag/CNTs are more effective sensors for the detection of these gases as compared to pristine non-decorated CNTs.

However, to the best of our knowledge, there is no theoretical report available in the literature on the adsorption of sulfide ion at the wall of pristine and –OH, –COOH and $–NH_2$ functionalized SWCNT. Therefore, we have used a quantum chemistry method to simulate the adsorption behavior of sulfide ion at the wall of pristine and functionalized SWCNT. Moreover, the structure and electronic properties of pristine and functionalized SWCNT through charge transfer and HOMO-LUMO energy gap have also been evaluated in the present DFT study.

## 2. Computational methodology

In the current research work, simulations ware performed to investigate the interaction of sulfide ion with the carbon nanotube. A nanotube modeler (Jcrystal Soft, 2005) was used to draw a structure of SWCNT for the computational simulations. All the DFT simulations were performed using Gaussian 09 software [37], while the results were analyzed through Gauss view 5.0 [38]. A DFT method called ωB97XD with suitable basis sets 6-31G (d,p) were used to simulate the optimized geometric parameters and charge transfer analysis of pristine and functionalized SWCNT interacting with sulfide ion. The electronic properties (IPs, EA, HOMO-LUMO energies, energy gap) and vibrational characteristics such as IR scaled frequencies (by applying a scaling factor of "0.9613") were calculated with the same level of theory. Similarly, the optical spectroscopic properties were calculated through UV–Vis–NIR spectral simulations by using the TD-DFT method and the spectra were analyzed through Gabedit 2.5.0 computer program.

The DFT method has proven to be one of the most accurate methods for the computation of the electronic structure of solids [39–44].

In order of to determine the stability of functionalized MWCNTs the binding energies of studied complexes are calculated. The binding energies were calculated according to the following equation: Binding energy per atom ($E_b$) values are computed by using equation (1) [45–47].

$$E_b = \frac{E_{complex} - (E_C + E_H + E_N + E_O)}{K} \quad (1)$$

Where, k is the total number of atoms present in MWCNT complex, $E_{complex}$ is the energy of functionalized MWCNT complex, whereas $E_C$, $E_H$, $E_N$ and $E_O$ represent the energies of carbon, hydrogen, nitrogen, and oxygen atoms, respectively.

Interaction energy is also calculated to evaluate the nature of interaction between functionalized SWCNTs and $S^{2-}$. The Interaction energy is calculated by employing equation (2):

$$E_{int} = E_{SWCNT-S2-}(E_{SWCNT} + E_{S2-}) \quad (2)$$

In equation (2), $E_{SWCNT\text{-}S2-}$ represents the energy of functionalized SWCNT-$S^{2-}$ complexes, $E_{SWCNT}$ denotes energy of functionalized SWCNT and $E_{S2-}$ presents energy of $S^{2-}$ (sulfide ion).

## 3. Results and discussions

### 3.1. Optimized geometric parameters

We have optimized the geometries of both pristine and edge/sidewall functionalized SWCNT interacting with sulfide ion, and these are labelled as SWCNT-$S^{2-}$, edge/sidewall OH+$NH_2$-SWCNT-$S^{2-}$, COOH+$NH_2$-SWCNT-$S^{2-}$. The optimized parameters including bond lengths and different angles (bond angles and dihedral angles) are listed in the Table 1.

#### 3.1.1. sWCNT-$S^{2-}$

The interaction behavior of sulfide ion with the SWCNT was studied by assuming three different interaction sites on CNTs. These sites could be a) top of the carbon atom in the tube, b) interaction with the bond between any two carbon atoms, c) interaction at the center of the hexagonal ring of the nanotube. Once the optimization was completed, it was observed that a stable structure is obtained when the sulfide ion has interacted with the bond between two carbon atoms (b) of SWCNT (illustrated in Fig. 1) Therefore, the further simulations were carried out with this stable optimized structure. The other less stable optimized geometries for SWCNT and sulfide ion complex (interacting at position a and c) are shown in supporting information (S1).

The geometry of pristine SWCNT was altered after the covalent interaction with sulfide ion. The $C_5$-$C_6$ bond length in the pristine SWCNT was simulated as 1.42 Å [48], however, after interaction with sulfide ion, the bond length ($C_5$-$C_{6)}$ was increased to 1.47 Å. The elongation in bond length in SWCNT-$S^{2-}$ was assumed to arise due to the interaction of analyte (sulfide ion) with SWCNT. The calculated intermolecular distance between $C_5$-$S^{2-}$ was 1.87 Å. Similarly, the simulated bond angle < $C_4C_5C_6$ of nanotube in pristine SWCNT was 120.17° and it was reduced to 117.60° in SWCNTs-$S^{2-}$. The reduction in the bond angle was attributed to the disruptions in π system in SWCNT upon interaction with sulfide ion in SWCNTs-$S^{2-}$. Moreover, the decrease in bond angle has promoted the transfer of charge from analyte (sulfide ion) to carbon atom of the SWCNT. The interaction of sulfide ion and SWCNTs not only affects the bond angle and bond distances but also causes changes in the dihedral angle < $C_3C_4C_5C_6$ from 180.00° to 178.62°. This change in dihedral angle was attributed to change in planarity of carbon atoms in SWCNT interacting with sulfide ion. These results indicated that the SWCNT presented better sensitivity towards the sulfide ion. However, to further improve the sensitivity of CNT towards the sulfide ion, the SWCNT were covalently edge/sidewall functionalized with the charge active functional groups like hydroxyl (OH) group, carboxyl (COOH) group and amine ($NH_2$) groups. For this purpose, we have simulated two types of functionalized system as OH+$NH_2$-SWCNT-$S^{2-}$ and COOH+$NH_2$-SWCNT-$S^2$.

**Table 1**
Optimized geometric parameters including bond lengths (Å), bond angles (degree) and dihedral angles (degree) for pristine and functionalized SWCNT interacting with sulfide ion.

| Optimized system | $dC_5$-S | $dC_5$-$C_6$ | $dC_4$-$C_5$ | <$C_6C_5S$ | <$C_4C_5C_6$ | <$C_3C_4C_5C_6$ | <$C_{14}C_4C_3C_{17}$ |
|---|---|---|---|---|---|---|---|
| SWCNT | ————— | 1.42 Å | 1.41 Å | ————— | 120.17° | 180.00° | 180.00° |
| SWCNT-$S^{2-}$ | 1.87 Å | 1.47 Å | 1.48 Å | 68.74° | 117.60° | 178.62° | 152.70° |
| OH+$NH_2$ -SWCNT-$S^{2-}$(Edge functionalized) | 1.86 Å | 1.48 Å | 1.49 Å | 67.87° | 117.44° | −179.73° | 153.39° |
| COOH+$NH_2$ -SWCNT-$S^{2-}$(Edge functionalized) | 1.86 Å | 1.48 Å | 1.49 Å | 67.49° | 117.91° | −178.89° | 153.61° |
| OH+$NH_2$ -SWCNT-$S^{2-}$(Sidewall functionalized) | 1.84 Å | 1.48 Å | 1.50 Å | 67.85° | 117.78° | 179.60° | 160.61° |
| COOH+$NH_2$ -SWCNT-$S^2$(Sidewall functionalized) | 1.83 Å | 1.49 Å | 1.50 Å | 67.42° | 117.77° | 179.73° | 161.66° |

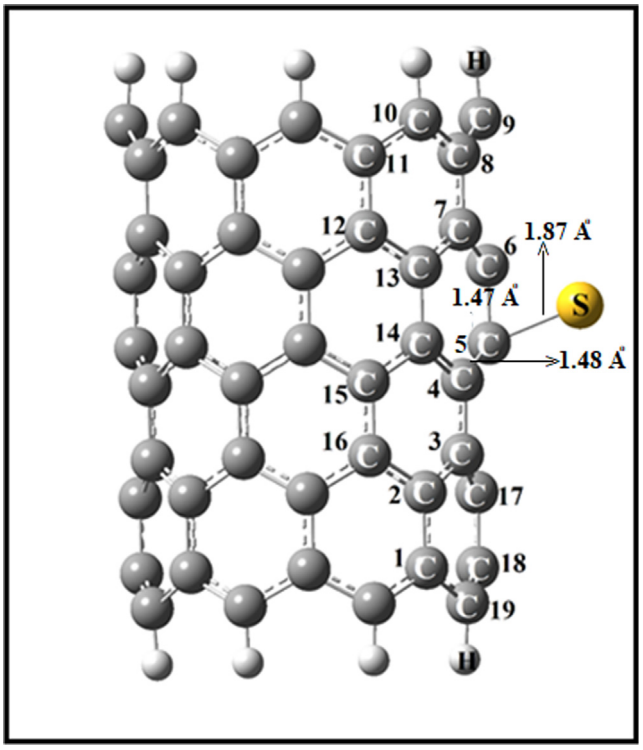


**Fig. 1.** Optimized geometry of SWCNT-$S^{2-}$ (sulfide interacting with the bond between two carbon atoms) simulated at ωB97XD/6-31G (d, p) level of theory.

### 3.1.2. oH+$NH_2$-SWCNT-$S^{2-}$

To evaluate the effect of OH and $NH_2$ groups on the geometry of SWCNT interacting with sulfide ion, we have covalently attached these groups to the SWCNT at the edge and at the sidewall of SWCNT interacting with sulfide ion. The optimized parameters of edge/sidewall functionalized OH+$NH_2$-SWCNT-$S^{2-}$ complex were then compared with those of the pristine SWCNT-$S^{2-}$. After complete optimization of edge/sidewall functionalized OH+$NH_2$-SWCNT-$S^{2-}$ (Fig. 2), the calculated ($C_5$-$C_6$) bond length in the vicinity of the adsorbed –OH was 1.48 Å for both edge and sidewall functionalized OH+$NH_2$-SWCNT-$S^{2-}$.

Similarly, the calculated $C_4$-$C_5$ bond length were 1.49 Å and 1.50 Å for edge and sidewall functionalized OH+$NH_2$-SWCNT-$S^{2-}$, respectively. These bond lengths were found greater than those of the pristine SWCNT and SWCNT-$S^{2-}$. However, the greater elongation in $C_4$-$C_5$ (1.50 Å) was observed near the adsorbed –$NH_2$ groups in sidewall functionalized OH+$NH_2$-SWCNT-$S^{2-}$ due to the interaction between $C_{17}$ and N. Similarly, the bond angle (<$C_4C_5C_6$) for the edge functionalized OH+$NH_2$-SWCNT-$S^{2-}$ was 117.60° whereas it is 117.38° for sidewall functionalized OH +$NH_2$-SWCNT-$S^{2-}$. The increase in bond lengths and decrease in bond angle of functionalized SWCNT with –OH and –$NH_2$ groups distorted the geometry of the SWCNT due to the rehybridization of carbon atoms of nanotubes from $sp^2$ to $sp^3$ upon C—O and C—N bonding with functional groups. The dihedral angles (Table 1) were also changed for both edge and sidewall functionalized OH +$NH_2$-SWCNT-$S^{2-}$.

Further, the simulated $C_5$-S bond length for edge functionalized OH+$NH_2$-SWCNT-$S^{2-}$ was 1.86 Å, which was smaller than that for the pristine SWCNT-$S^{2-}$ (1.87 Å). However, the $C_5$-S bond length for sidewall functionalized OH+$NH_2$-SWCNT-$S^{2-}$ was further decreased to 1.84 Å. Therefore, this decrease in $C_5$-S bond length clearly revealed that the sulfide ion has shown better interaction with nanotube in sidewall functionalized OH+$NH_2$-SWCNT-$S^{2-}$ due to the small distance of interaction between the electronegative functional group and the carbon atom of SWCNT to which sulfide ion is attached. Similarly, the decrease in < $C_6C_5S$ bond angle was observed for both edge functionalized (67.87°) and sidewall functionalized (67.85°) OH+$NH_2$-SWCNTs-$S^{2-}$. Therefore, the decrease in < $C_6C_5S$ bond angle have promoted the charge transfer from the sulfide ion to the SWCNT.

### 3.1.3. cOOH-$NH_2$-SWCNT-$S^{2-}$

The combined effect of COOH and $NH_2$ groups at the edge and sidewall of SWCNT was analyzed by optimizing the geometry of COOH+$NH_2$-SWCNT-$S^{2-}$ (Fig. 3) and compared the results with those of the pristine SWCNT-$S^{2-}$. As shown in Table 1, the calculated $C_5$-$C_6$ bond length in the vicinity of the adsorbed COOH was 1.48 Å for edge functionalized COOH+$NH_2$-SWCNT-$S^2$, while it was increased to 1.49 Å for the sidewall functionalized COOH +$NH_2$-SWCNT-$S^{2-}$. Similarly, the bond lengths $C_4$-$C_5$ in the vicinity of $NH_2$ group were 1.49 Å and 1.50 Å for edge and sidewall functionalized COOH+$NH_2$ SWCNTs-$S^{2-}$, respectively. This increase in bond lengths up to 1.50 Å has revealed that the sidewall functionalization of COOH and $NH_2$ has greater effect on the geometry of SWCNT interacting with sulfide ion. Also, the bond angles < $C_4C_5C_6$ for edge functionalized COOH+$NH_2$-SWCNTs-$S^{2-}$ and sidewall functionalized COOH+$NH_2$-SWCNTs-$S^2$ were 117.60° and 117.38°, respectively. The increase in bond lengths and decrease in bond angle of functionalized SWCNT with COOH and $NH_2$ groups distorted the geometry of the SWCNT due to the rehybridization of carbon atoms of nanotubes from $sp^2$ to $sp^3$ upon C—O and C—N bonding with functional groups The dihedral angles (Table 1) were also changed for both edge and sidewall functionalized COOH +$NH_2$-SWCNTs-$S^{2-}$.

Similarly, the $C_5$-S simulated bond length for the edge functionalized COOH+$NH_2$ -SWCNTs-$S^{2-}$ was 1.84 Å which was smaller than that for the pristine SWCNTs-$S^{2-}$(1.87 Å), however, the $C_5$-S bond length was further decreased to 1.83 Å by the sidewall functionalization of SWCNTs-$S^{2-}$ with COOH and $NH_2$. This is attributed to the greater interaction between carbon atom of SWCNT and highly electronegative oxygen atom of COOH group which in turn greatly promoted the interaction between sulfide ion and SWCNT. Moreover, upon sidewall functionalization of SWCNT with COOH and $NH_2$ groups, the nanotube has shown greater interaction towards sulfide ion by making two sigma S—C bonds between carbon atoms of SWCNT and sulfide ion. The greater interaction of SWCNT and

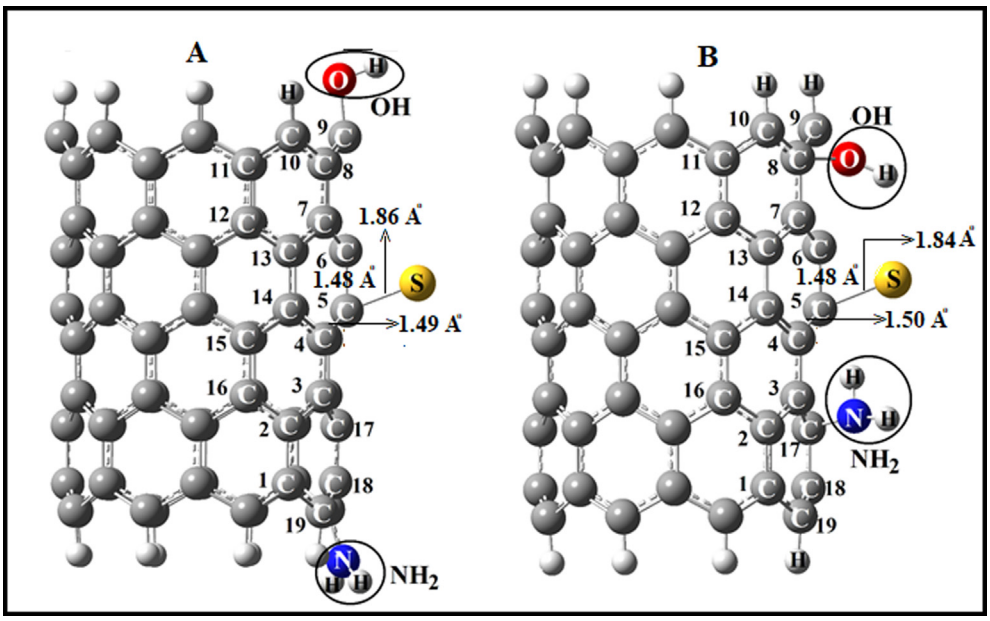


**Fig. 2.** Optimized geometries of edge functionalized OH+$NH_2$-SWCNT-$S^{2-}$ A) and sidewall functionalized OH+$NH_2$-SWCNT-$S^{2-}$ B) simulated at ωB97XD/6-31G (d, p) level of theory.

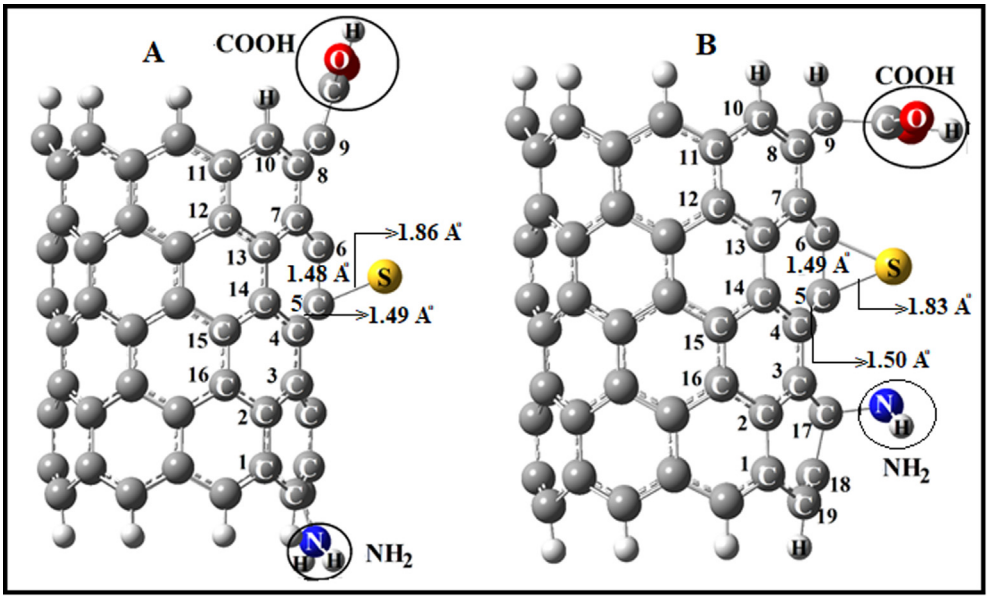


**Fig. 3.** Optimized geometries of edge functionalized COOH+$NH_2$-SWCNT-$S^{2-}$ A) sidewall functionalized COOH+$NH_2$-SWCNT-$S^{2-}$ B) simulated at ωB97XD/6-31G (d,p) level of theory.

sulfide ion may also be attributed to the sufficiently small distance of interaction between the functional groups and carbon atom of the tube bonded to the analyte. Similarly, the simulated < $C_6C_5S$ bond angle for edge COOH+$NH_2$-SWCNTs-$S^{2-}$ was 67.87° whereas it is 67.85° for sidewall functionalized COOH+$NH_2$-SWCNT-$S^{2-}$.

From all the optimized parameter (Table 1), it was revealed that the sidewall functionalized COOH+$NH_2$-SWCNT has shown greater interaction with sulfide ion due to the presence of COOH groups in the vicinity of C—S bond. This group tend to attract electron density from SWCNT, which in turn has withdrawn charges from sulfide ion by making two sigma bonds between sulfide ion and carbon atom of SWCNT.

- $dC_5$-S**:** Bond distance between $C_5$ of single wall carbon nanotube and sulfide ion.
- $dC_5$-$C_6$**:** Bond distance between $C_5$ and $C_6$ of single wall carbon nanotube.
- $Dc_4$-$C_5$**:** Bond distance between $C_6$ and $C_7$ of single wall carbon nanotube.
- <$C_6C_5S$**:** Bond angle $C_6$, $C_5$ of single wall carbon nanotube and sulfide ion.
- <$C_8C_7C_{13}C_{14}$**:** Dihedral angle $C_8$, $C_7$, $C_{13}$, and $C_{14}$ of single wall carbon nanotube.
- <$C_{14}C_4C_3C_{17}$**:** Dihedral angle $C_{14}$, $C_4$, $C_3$, and $C_{17}$ of single wall carbon nanotube. (See Fig. 1).

### 3.2. Binding energy and stability

The calculated binding energy ($E_b$) and the interaction energy ($E_{int}$) values are given in Table 2. The binding energy values per atom for simple SWCNT is maximum i.e., −8.00 eV. Whereas for functionalized SWCNT the binding energy values are observed in the range of −7.84 eV to −7.95 eV. The higher binding energy values reveal that the considered functionalized SWCNT complexes are stable. Binding energy results further reveal that OH+$NH_2$-SWCNT are more stable (both edge and sidewall functionalized) as compared to COOH+$NH_2$-SWCNT complex. Furthermore, the maximum $E_b$ value in case of simple SWCNT indicates that non-functionalized MWCNTs are more stable. The interaction energy results also reveal that adsorption of $S^{2-}$ over non-functionalized SWCNT resulted in most stable SWCNT-$S^{2-}$ complex with $E_{int}$ of −7.53 eV. Whereas for functionalized SWCNT the interaction energy values observed are in the range of −5.59 eV to −6.45 eV. High binding energy values per atom indicate higher stability of our studied functionalized SWCNT-$S^{2-}$ complexes.

### 3.3. Charge transfer analysis

Charge transfer (taking place between interacting atoms, ions, or molecules) is an important phenomenon that describes the electronic structure, conductivity, and sensitivity of the substrate towards the analyte. In carbon nanotubes (CNTs), transfer of charge can also be defined as the sensing capability of the nanotubes towards the interacting molecules. Moreover, the overall charge transfers between CNTs and analytes can determine the type of doping, either *n*-type or p-type. Therefore, to determine the sensitivity of SWCNT towards sulfide ion, we have simulated the NBO and Mulliken charges (summarized in Table 3) for both pristine and functionalized SWCNT interacting with sulfide.

Initially, sulfide ion ($S^{2-}$) bears charge of −2.000 $e^-$ and pristine SWCNT exhibits 0.000 $e^-$. However, upon interaction of sulfide ion with SWCNT, appreciable charge transfer is observed. Based on NBO analysis, in case of SWCNT-$S^{2-}$, the remaining charge on sulfide ion is about −0.033 $e^-$, which means a charge of about −1.967 $e^-$ is transferred by sulfide ion to pristine SWCNT. Similarly, in case of edge functionalized OH+$NH_2$-SWCNT-$S^{2-}$ and COOH +$NH_2$-SWCNT-$S^{2-}$, NBO charges observed on sulfide ion are −0.034 $e^-$ and 0.042 $e^-$, respectively. NBO charges clearly indicate that charges of −1.966 $e^-$ and −2.042 $e^-$ are transferred from sulfide ion to edge functionalized OH+$NH_2$-SWCNT and COOH+$NH_2$-SWCNT, respectively. Similarly, upon sidewall functionalization of OH+$NH_2$-SWCNT-$S^{2-}$ and COOH+$NH_2$-SWCNT-$S^{2-}$, sulfide ion transfers charge of −2.059 $e^-$ and −2.115 $e^-$ to the functionalized SWCNT. The higher charge transfer from sulfide ion to sidewall functionalized SWCNTs is attributed to the covalent interaction of electronegative functional groups attached at the sidewall of SWCNT near the carbon atom (directly attached to the sulfide ion).

Similarly, Mulliken charge analysis also shows the comparable results with that of NBO analysis. In case of Mulliken charge analysis, the charge is transferred from sulfide ion to pristine SWCNT and functionalized SWCNT in all studied complexes. The highest charge transfer in this case is also observed for sidewall functionalized COOH+$NH_2$-SWCNT-$S^{2-}$ (-1.976 $e^-$), whereas the least Mulliken charge of −1.859 $e^-$ is transferred in case of both SWCNT-$S^{2-}$ and edge functionalized. OH+$NH_2$-SWCNT.

The charge transfers and sensitivity of SWCNT towards sulfide ion was further simulated by the edge/sidewall functionalization of SWCNT-$S^{2-}$ with most electronegative COOH and $NH_2$ groups. NBO and Mulliken charge analysis reveal that higher amount of charge is transferred by sulfide ion to the sidewall functionalized COOH+$NH_2$-SWCNT as compared to the pristine SWCNT-$S^{2-}$ and other functionalized SWCNTs, which can be attributed to the most electronegative COOH and $NH_2$ groups covalently attached in the vicinity of sulfide ion. Therefore, based on NBO charge analysis, sidewall functionalized COOH+$NH_2$-SWCNT has shown a higher sensitivity towards sulfide ion.

**Table 2**
Binding energy/atom ($E_b$) of studied functionalized SWCNTs and interaction energy ($E_{int}$) between the functionalized SWCNTs and $S^{2-}$.

| Complex | $E_b$ (eV) | Complex | $E_{int}$ with $S^{2-}$ (eV) |
|---|---|---|---|
| SWCNT | −8.00 | SWCNT-$S^{2-}$ | −7.53 |
| OH+$NH_2$-SWCNT (Edge functionalized) | −7.94 | OH+$NH_2$-SWCNT-$S^{2-}$ (Edge functionalized) | −5.59 |
| COOH+$NH_2$-SWCNT (Edge functionalized) | −7.84 | COOH+$NH_2$-SWCNT-$S^{2-}$ (Edge functionalized) | −6.45 |
| OH+$NH_2$-SWCNT (Sidewall functionalized) | −7.95 | OH+$NH_2$-SWCNT-$S^{2-}$ (Sidewall functionalized) | −6.14 |
| COOH+$NH_2$-SWCNT (Sidewall functionalized) | −7.86 | COOH+$NH_2$-SWCNT-$S^{2-}$ (Sidewall functionalized) | −6.14 |

**Table 3**
NBO and Mulliken charge analysis of pristine and functionalized SWCNT interacting with sulfide at the ωB97XD/6-31G (d, p) level of theory.

| Complexes | Q(NBO) | Q(Mulliken) | Q(CHELPG) |
|---|---|---|---|
| SWCNT-$S^{2-}$ | −0.033 | −0.141 | −0.592 |
| OH+$NH_2$-SWCNT-$S^{2-}$ (Edge functionalized) | −0.034 | −0.141 | −0.672 |
| COOH+$NH_2$-SWCNT-$S^{2-}$ (Edge functionalized) | 0.042 | −0.080 | −0.609 |
| OH+$NH_2$-SWCNT-$S^{2-}$ (Sidewall functionalized) | 0.059 | −0.060 | −0.585 |
| COOH+$NH_2$-SWCNT-$S^{2-}$ (Sidewall functionalized) | 0.115 | −0.024 | −0.476 |

### 3.4. Infra-red spectroscopic simulation

The infra-red (IR) spectroscopy is a simple and reliable technique which is used to study the structural properties and the identifications of functional groups associated with both organic and inorganic compounds. For this purpose, we have simulated IR spectra of pristine and edge/sidewall functionalized SWCNT interacting with sulfide ion using DFT method. The IR spectrum for pristine SWCNT interacting with sulfide ion is shown in Fig. 4 (A). Similarly, the simulated spectra for sidewall functionalized OH+$NH_2$-SWCNT-$S^{2-}$ and sidewall functionalized COH+$NH_2$-SWCNT-$S^{2-}$ are illustrated in Fig. 4 (B) and Fig. 4 (C), while the IR spectra for edge functionalized OH+$NH_2$-SWCNT-$S^{2-}$ and OH +$NH_2$-SWCNT-$S^{2-}$ are shown in the supporting information (S2, S3) Generally, the theoretically simulated frequencies are overestimated due to harmonic models, therefore, a scaling factor of "0.9613" was applied to the simulated frequencies to get the scaled frequencies. The scaled and unscaled frequencies in correlation with the reported experimental values are listed in Table 4. The DFT simulated bands at 3047–3065 $cm^{-1}$ were attributed to the C—H stretching vibrations in the SWCNT interacting with sulfide ion. However, the C—H stretching vibrations were shifted to lower frequencies at around 2994–3041 $cm^{-1}$ and 2941–3037 $cm^{-1}$ for OH+$NH_2$-SWCNT-$S^{2-}$ and COOH+–$NH_2$-SWCNT-$S^{2-}$-, respectively. These bands could be attributed to the sidewall covalent interaction of the OH, COOH and $NH_2$ groups with the SWCNT. Similarly, a peak calculated at 1541–1600 $cm^{-1}$ was assigned to the C—C stretching of SWCNT hexagonal skeleton which was experimentally confirmed to originate from the $sp^2$ bonded carbon at 1530–

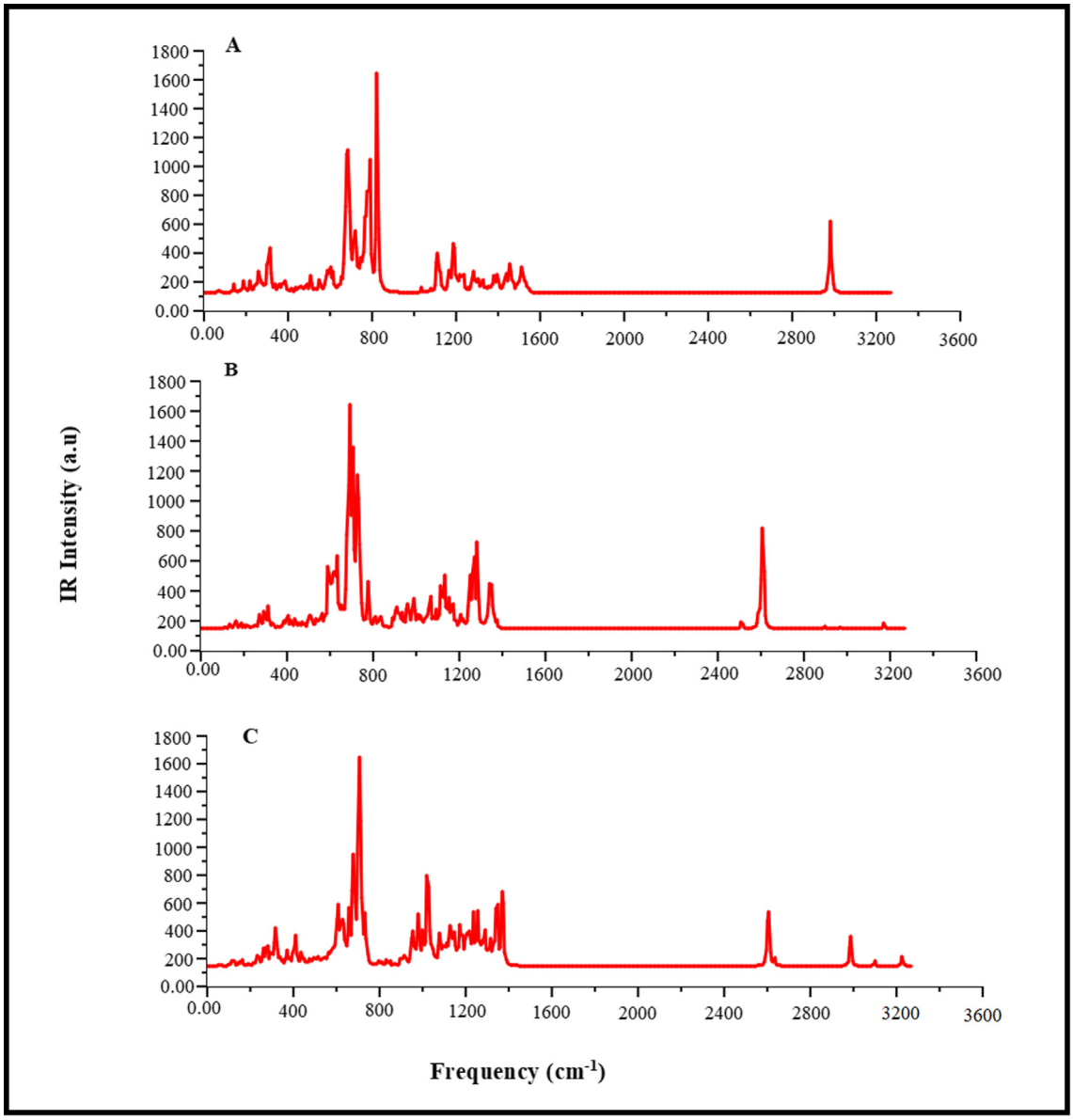


**Fig. 4.** Calculated IR spectrum of SWCNT-$S^{2-}$ **(A)** OH+$NH_2$-SWCNT-$S^{2-}$ **(B)**, COOH+$NH_2$-SWCNT-$S^{2-}$ **(C)**, simulated at ωB97XD/6-31G (d, p) level of theory.

**Table 4**
Scaled and unscaled calculated IR frequencies ($cm^{-1}$) of pristine and functionalized SWCNT interacting with sulfide ion at ωB97XD/6-31G (d, p) level of theory (Experimental for comparison).

| Simulated IR ($cm^{-1}$) | | Experimental IR ($cm^{-1}$) | Probable assignment | Ref. |
|---|---|---|---|---|
| Unscaled | Scaled | | | |
| 3938 | 3785 | 3700–3800 | *ν* O—H of surface OH group | [48] |
| 3856 | 3706 | 3700–3200 | *ν* O—H of surface COOH group | [51] |
| 3514–3609 | 3378–3469 | 3420 | *ν* N—H of surface –$NH_2$ group | [52] |
| 3170–3189 | 3047–3065 | 2800–3000 | *ν* C—H of pristine CNT edges | [53] |
| 3115–3164 | 2994–3041 | – | *ν* C—H of CNT-OH+$NH_2$ | |
| 3060–3160 | 2941–3037 | – | *ν* C—H of CNT-COOH+$NH_2$ | |
| 1876 | 1803 | 1700–1800 | *ν* C=O of COOH group | [54] |
| 1669–1675 | 1604–1610 | – | β H—N—H of surface –$NH_2$ group | |
| 1604–1655 | 1541–1600 | 1530–1580 | $\nu_{as}$ –$COO^-$ in CNT-COOH | [55] |
| 1441–1300 | 1385–1249 | 1100–1200 | *ν* C=C of CNT backbone | [56] |
| 804–895 | 772–860 | – | β C—H of CNT back bone | [54] |
| 668 | 642 | 600–700 | *ν* C—S in pristine CNT | [48] |
| 680 | 653 | – | *ν* C—S in CNT-OH+$NH_2$ | |
| 701–706 | 673–678 | – | *ν* C—S—C in CNT-COOH+$NH_2$ | |

*ν*: stretching, as: asymmetric, β: bending.

1580 $cm^{-1}$ [49]. It was also observed that in the functionalized SWCNT, the O—H stretching vibrations in both hydroxyl and carboxyl were simulated at 3785 $cm^{-1}$ and 3706 $cm^{-1}$, respectively, while the N—H stretching in amine was calculated to appear at 3378–3469 $cm^{-1}$. A peak calculated around 1604–1610 $cm^{-1}$ was assigned to the N—H bending vibration of $NH_2$ group. However, such peaks were not appearing in the pristine SWCNT interacting with sulfide. Additionally, the C—S vibrational frequency of SWCNT-$S^{2-}$ calculated at 642 $cm^{-1}$ was in better agreement with the experimentally reported frequency at 600–700 $cm^{-1}$ [50]. However, the C—S vibrational frequency was shifted to 653 $cm^{-1}$ in the SWCNT-$S^{2-}$–OH+–$NH_2$ while in the SWCNT-$S^{2-}$–COOH+–$NH_2$ a C—S—C stretching was observed around 673–678 $cm^{-1}$. This shifting of C—S stretching vibrations towards higher frequency was attributed to the greater interaction and shorter bond distance between the sulfide ion and carbon of functionalized SWCNNT.

### 3.5. UV–Vis–NIR spectral simulations

UV–Vis–NIR spectroscopy is an essential analytical tool that determines the various optical properties of solids and liquids. It is used to characterize the semiconductors, glass and crystalline solids. UV–Vis–NIR could be operated in an optical range of 0.00 to 3.00 eV. The transitions recorded in this range correspond to an overtone combined with the mid IR vibrational mode [57]. Since like other crystalline solids, carbon nanotubes (CNTs) are also UV–Vis–NIR active due to the one dimensional van Hove singularities (non- smooth points) energy levels with high density of states which are responsible for the additional adsorption peaks [58]. Theoretically, it has also been reported that the SWCNT possess large absorption bands due to the transition between spikes like density of states [59].

Further depending on the diameter and chirality, the SWCNTs can be differentiated into two types of namely semiconductors and metallic. Therefore, due to inner band transitions, the van Hove singularities for semiconductor SWCNTs can be divided into two set of pairs. The first pair of van Hove singularities is known $S_{11}$ band, and the second pair of singularities is called as $S_{22}$ band. Likewise, the inter band transitions in metallic SWCNT for the first and second pair of singularities can be designated by $M_{11}$ and $M_{22}$, respectively [60]. Further, upon functionalization and external doping of the sidewall or open ends of SWCNT, the electronic and the optical properties are completely altered due to the localizations of electron and decline in the singularities [61].

For this purpose, we have simulated the UV–Vis–NIR absorption spectra of both pristine and functionalized SWCNT with and without sulfide ion using TD-DFT method. In all studied cases, the peaks are shifted towards longer wavelength or lower energy upon adding sulfide ion (see Figs. 5 & 6). The oscillator strength was functioned as absorbance in the UV–Vis–NIR spectra, simulated at TD-DFT method. The simulated peak at 0.40 eV (Figs. 5 & 6) could be assigned to the first inter band transition ($ES_{11}$) in the pristine SWCNT-$S^2$ based on their transition energy. Likewise, the peak simulated at 1.03 eV was assigned to the second inter band transition (E $S_{22}$) in the pristine SWCNT-$S^2$. These bands could be assigned to the semiconducting properties of pristine SWCNT which were comparable with the experimentally observed peaks [62]. However, upon functionalization of SWCNT with OH, COOH and $NH_2$ groups, the $S_{11}$ peaks vanished off and some new bands were appeared around 0.60–0.65 eV for edge functionalized OH +$NH_2$-SWCNT-$S^{2-}$ and COOH+$NH_2$-SWCNT-$S^{2-}$, which could be assigned to the first inter band transition ($M_{11}$) in metallic SWCNT [60]. Similarly, the peak appeared at 1.30 eV in edge functionalized OH+$NH_2$-SWCNT-$S^{2-}$ (depicted in Fig. 5) was assigned to second pair of singularities designated as $M_{22}$ of metallic carbon nanotube, while this peak was further shifted to 1.47 eV with higher intensity in edge functionalized COOH+$NH_2$-SWCNT-$S^{2-}$ as shown in Fig. 6.

Thus, due to the appearance of $M_{11}$ and $M_{22}$, the energy gaps $ES_{11}$ and $ES_{22}$ were decreased, which suggested that the electronic and UV–Vis–NIR absorption properties of SWCNT was altered by edge functionalization with OH, COOH and $NH_2$ groups, which has promoted the metallic conductivities of SWCNT and thus the edge functionalized nanotube was sensitive towards sulfide ion. Further, the metallic conductivity and sensitivity of SWCNT towards sulfide ion was also simulated by the sidewall functionalization of SWCNT with OH, COOH and $NH_2$ groups. For this purpose, the simulated spectrum for sidewall functionalized OH +$NH_2$-SWCNT-$S^{2-}$ is illustrated in Fig. 5 while, for sidewall functionalized COOH+$NH_2$-SWCNT-$S^{2-}$, the spectrum is displayed in Fig. 6. From these spectra it was observed that the peaks related to first inter band transition ($M_{11}$) were further shifted to higher energy and an intense peak at 1.48 eV nm was observed for both sidewall functionalized OH+$NH_2$-SWCNT-$S^{2-}$ and COOH+$NH_2$-SWCNT-$S^{2-}$. Similarly, the peaks calculated at 1.82 eV and 1.85 eV for OH+$NH_2$-SWCNT-$S^{2-}$ and COOH+$NH_2$-SWCNT-$S^{2-}$, respectively, were assigned to the second pair of inter band transition of metallic CNTs [57].

From all these results, it was clear that the metallic conductivities in sidewall functionalized OH+$NH_2$-SWCNT-$S^{2-}$ and COOH +$NH_2$-SWCNT-$S^{2-}$ was further increased, due to the inter band transitions at lower wavelength than that of edge functionalized OH +$NH_2$-SWCNT-$S^{2-}$ and COOH+$NH_2$-SWCNT-$S^{2-}$. In this way, the charge transfer was highly promoted in sidewall functionalized SWCNT, which has greatly increased the sensitivity of nanotube towards sulfide ion.

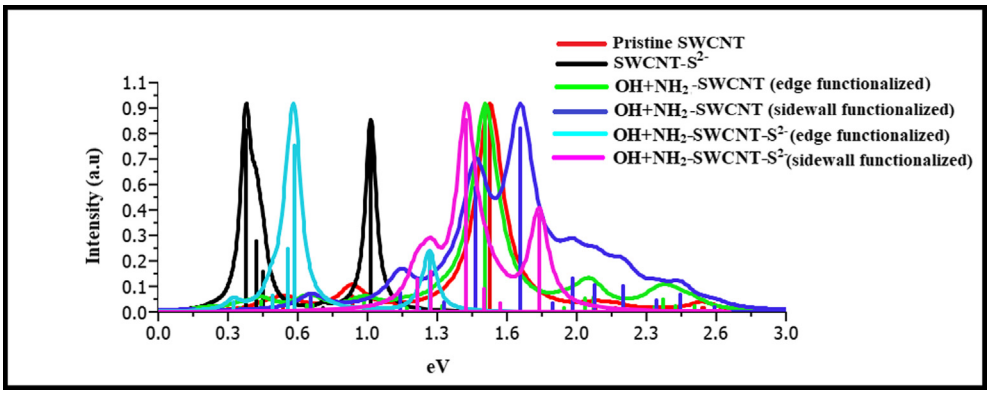


**Fig. 5.** UV–Vis–NIR spectra of pristine and edge/sidewall functionalized OH+$NH_2$-SWCNT interacting with and without sulfide ion at TD-DFT method.

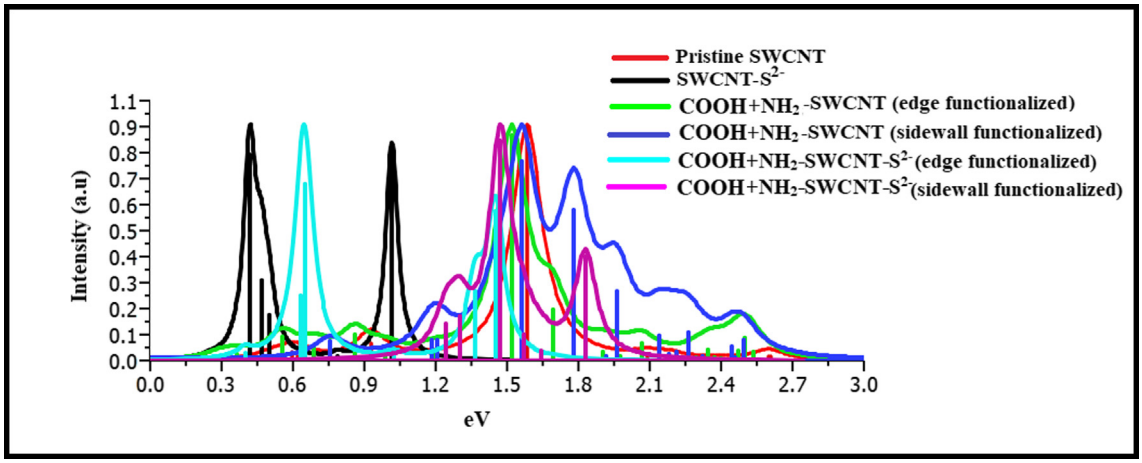


**Fig. 6.** UV–Vis–NIR spectra of pristine and edge/sidewall functionalized COOH+$NH_2$-SWCNT interacting with and without sulfide ion at TD-DFT method.

### 3.6. HOMO-LUMO orbital simulation

Highest occupied molecular orbitals (HOMOs) and lowest unoccupied molecular orbitals (LUMOs) collectively known as FMOs (frontier molecular orbitals) are key factors in quantum mechanics to provide information about the interaction between the analyte and the sensors [63]. These orbitals are the basic tools to explain the electronic, optical properties of conjugated systems like polymers and CNTs. A molecule will be considered as an unstable if its HOMO energies are high. Similarly, a low HOMO-LUMO energy gap indicates the reactivity of a chemical system [64]. The HOMO-LUMO (H-L) gap interconnected to the special types of approximations known as "frozen orbital approximation" where the excited states energies are calculated with respect to the orbitals of the ground state [65]. In this regard, we have simulated the HOMO-LUMO orbitals energy of both pristine (Fig. 7) and functionalized SWCNT (Fig. 8) and (Fig. 9) interacting with sulfide ion and the simulated HOMO-LUMO energies, IPs, EAs and band gas are listed in Table 5. The calculated HOMO and LUMO energies of pristine SWCNT were −7.39 eV and 6.,81 eV, respectively and the H-L gap was 0.58 eV. However, to increase the sensitivity of SWCNT towards sulfide ion, we have covalently functionalized the SWCNT-$S^{2-}$ with OH, COOH and $NH_2$ functional groups. After interaction with sulfide ion, the calculated HOMO energy of SWCNT-$S^{2-}$ was −7.22 eV and LUMO energy was −6.68 eV, therefore, the H-L gap was calculated as 0.54 eV.

For this purpose, after the edge functionalization of SWCNT-$S^{2-}$ with OH and $NH_2$ groups, the calculated HOMO energy was −7.20 eV and the LUMO energy was −6.72 eV therefore, the H-L gap for OH+$NH_2$-SWCNT-$S^{2-}$ was 0.48 eV. This H-L gap was lower than that was calculated for pristine SWCNT-$S^{2-}$ (0.54 eV). Similarly, the calculated HOMO energy of sidewall functionalized OH +$NH_2$-SWCNT-$S^{2-}$ was −7.07 eV where LUMO energy was −6.82 eV with the calculated H-L gap of 0.25 eV. The decrease in energy gap of sidewall functionalized OH+$NH_2$-SWCNT-$S^{2-}$ was attributed to the attachment of electronegative OH and $NH_2$ groups in the neighborhood of the sulfide ion attached. Similarly, the sensitivity of SWCNT towards sulfide ion was also simulated by the

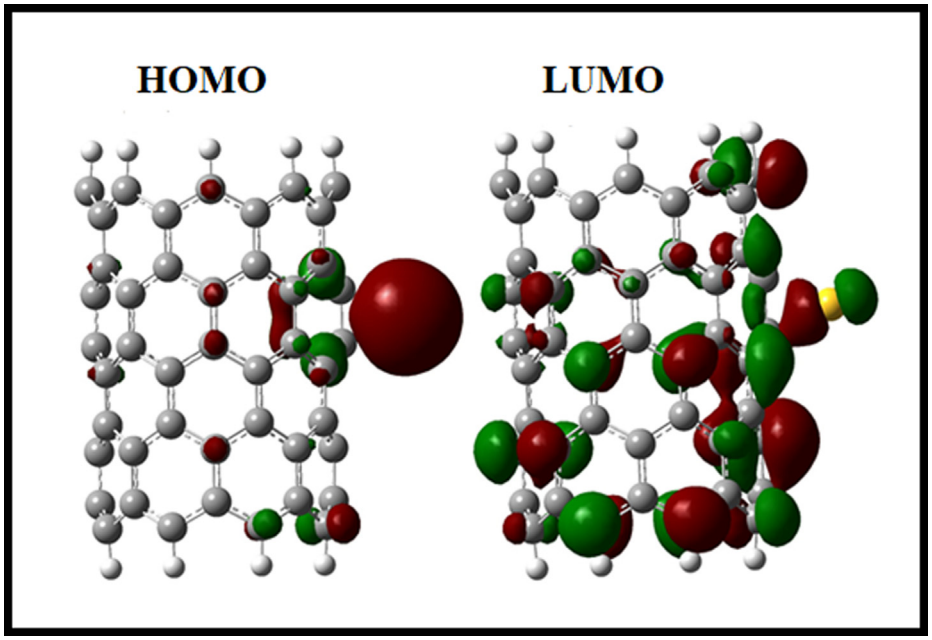


**Fig. 7.** Frontier molecular orbitals structure of SWCNT-$S^{2-}$ simulated at ωB97XD/6-31G (d, p) method.

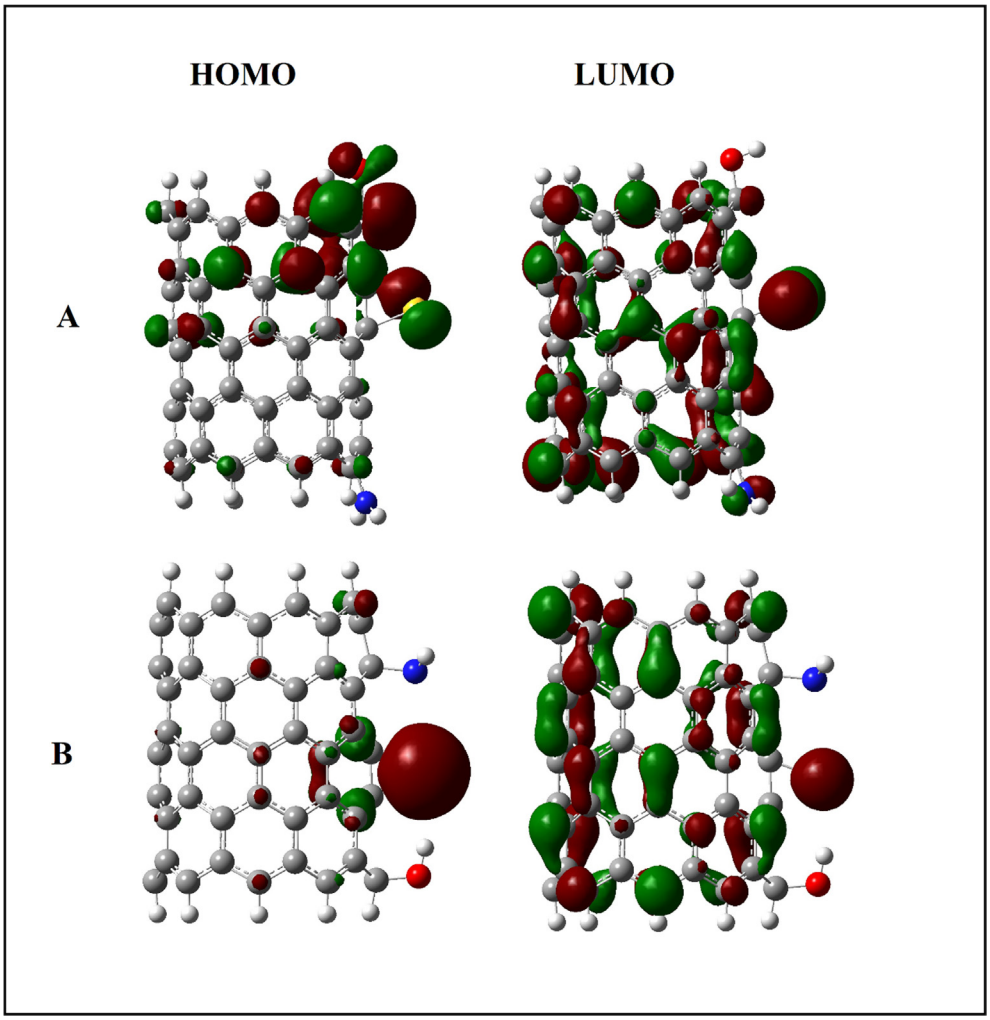


**Fig. 8.** Frontier molecular orbitals structure of A) edge functionalized OH+$NH_2$-SWCNT-$S^{2-}$ B) sidewall functionalized OH+$NH_2$-SWCNT-$S^{2-}$ simulated at ωB97XD/6-31G (d, p) method.

edge/sidewall functionalization of SWCNT-$S^{2-}$ with COOH and $NH_2$ groups. Therefore, after edge functionalization of COOH+$NH_2$-SWCNT-$S^{2-}$, the calculated HOMO and LUMO energies were −7.21 eV and −6.82 eV, respectively, and the H-L gap calculated for this system was 0.39 eV. Similarly, the HOMO energy calculated for the sidewall functionalized COOH+$NH_2$-SWCNT-$S^{2-}$ was −7.19 eV and the LUMO energy was −6.97 eV and therefore, the H-L gap was further reduced to 0.22 eV. This noticeable decrease in sidewall functionalized COOH+$NH_2$-SWCNT-$S^{2-}$ was due to the introduction of most electronegative COOH and $NH_2$ groups at the sidewall of SWCNT in the vicinity of sulfide ion. These functional groups tend to produce positive carbon active sites in the SWCNT through inductive effect. From all the calculated HOMO-LUMO energies and H-L gap, it was revealed the sidewall functionalized OH+$NH_2$-SWCNT-$S^{2-}$ and COOH+$NH_2$-SWCNT-$S^{2-}$ are more reactive towards sulfide ion. However, due to the lower H-L gap, the sidewall functionalized COOH+$NH_2$-SWCNT-$S^{2-}$ could be an efficient sensor for sulfide ion.

Furthermore, according to the Koopmans theorem [66] the IPs and EAs for both pristine and functionalized SWCNT interacting with sulfide ion were simulated from the negative of the HOMO and LUMO orbitals energy. As can be seen in Table 5 that the calculated IPs and EAs are positive values which will be helpful in future for both experimental and theoretical analysis.

## 4. Conclusions

The structural and electronic properties of pristine and edge/sidewall functionalized SWCNT and their sensitivity towards sulfide ion was investigated by performing DFT studies. After functionalization of SWCNT with functional groups like OH, COOH and $NH_2$, the geometric parameters and electronic properties have changed, which greatly enhanced the sensing ability of SWCNT towards sulfide ion. However, the geometry changes and interaction with sulfide ion was more prominent by the sidewall functionalization of SWCNT with COOH+$NH_2$ groups. Similarly, according to NBO analysis, a greater amount of charge was transferred sulfide ion to SWCNT in the case of sidewall functionalized COOH+$NH_2$-SWCNT-$S^{2-}$. The change in vibrational frequencies and the greater interaction between COOH+$HN_2$-SWCNT and analyte (sulfide ion) was also advocated from the IR spectral analysis, where C—H stretching of SWCNT was decreased and C—S stretching was observed to increase upon functionalization. The UV–Vis–NIR simulations was also illustrated the change in optical properties as well as the increase in metallic conductivities of SWCNT when functionalized with COOH, OH and $NH_2$ groups. However, a greater metallic character was observed in sidewall functionalized COOH +$NH_2$-SWCNT-$S^{2-}$. Similarly, the FMOs analysis and the trend in decrease of energy band gap from pristine to OH+$NH_2$-SWCNT-$S^{2-}$ and COOH-$NH_2$-SWCNT-$S^{2-}$ was also indicated the change in

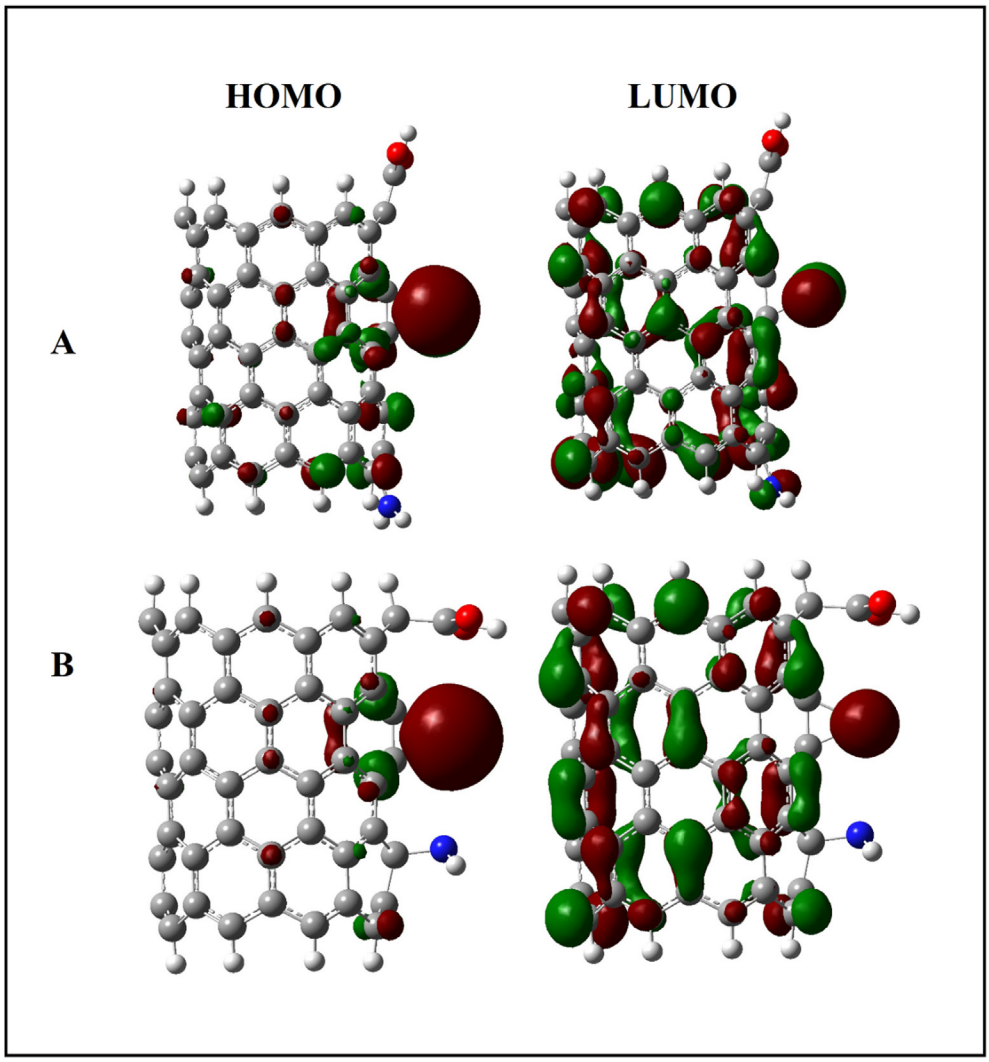


**Fig. 9.** Frontier molecular orbitals structure of A) edge functionalized COOH+$NH_2$-SWCNT-$S^{2-}$ B) sidewall functionalized COOH+$NH_2$-SWCNT-$S^{2-}$ simulated at ωB97XD/6-31G (d, p) method.

**Table 5**
HOMOs, LUMOs, IPs, EAs and Energy band gap simulated at ωB97XD/6-31G (d, p) level of theory.

| System | IPs | EAs | HOMO | LUMO | Energy gap (eV) |
|---|---|---|---|---|---|
| SWCNT | 7.39 | 6.81 | −7.39 | −6.81 | 0.58 |
| SWCNT-$S^{2-}$ | 7.22 | 6.68 | −7.22 | −6.68 | 0.54 |
| OH+$NH_2$-SWCNT-$S^{2-}$ (Edge functionalization) | 7.20 | 6.72 | −7.20 | −6.72 | 0.48 |
| OH+$NH_2$-SWCNT-$S^{2-}$(Sidewall functionalization) | 7.07 | 6.82 | −7.07 | −6.82 | 0.25 |
| COOH+$NH_2$-SWCNT-$S^{2-}$(Edge functionalized) | 7.21 | 6.82 | −7.21 | −6.82 | 0.39 |
| COOH+$NH_2$-SWCNT-$S^{2-}$ (Sidewall functionalization) | 7.19 | 6.97 | −7.19 | −6.97 | 0.22 |

electronic properties of functionalized SWCNT. The low energy band gap in sidewall functionalized COOH-$NH_2$-SWCNT-$S^{2-}$ has suggested that the SWCNT has shown a greater sensitivity towards sulfide ion, when it was sidewall functionalized with COOH and $NH_2$ groups.

Conclusively, all these results clearly demonstrated that the geometric, optical, and electronic properties of SWCNT was altered by the edge/sidewall covalent functionalization with functional groups such as COOH, OH and $NH_2$. However, a prominent change in structure and electronic properties of SWCNT upon sidewall functionalization with COOH and $NH_2$ was revealed that the sidewall functionalized COOH-$NH_2$-SWCNT-$S^{2-}$ has shown a greater sensitivity towards sulfide ion.

*CRediT authorship contribution statement*

**Sania Bibi:** Conceptualization, Investigation, Writing – original draft. **Sehrish Sarfaraz:** Software, Validation. **Muhammad Yar:** Visualization. **Muhammad Iqbal Zaman:** Methodology, Supervision. **Abdul Niaz:** Visualization, Investigation. **Ayesha Khan:** Software. **Muhammad Ali Hashmi:** Validation, Visualization. **Khurshid Ayub:** Supervision, Writing – review & editing.

## Data availability

Data will be made available on request.

## Declaration of Competing Interest

The authors declare that they have no known competing financial interests or personal relationships that could have appeared to influence the work reported in this paper.

## References


[1] S. Iijima, Helical microtubules of graphitic carbon, Nature 354 (6348) (1991) 56–58.
[2] P.K. Naidu, N.V. Pulagara, R.S. Dondapati, Carbon nanotubes in engineering applications, Prog. Nanotechnol. Nanomater. 3 (4) (2014) 79.
[3] R.S. Ruoff, D.C. Lorents, Mechanical and thermal properties of carbon nanotubes, Carbon 33 (7) (1995) 925–930.
[4] G. Van Lier, C. Van Alsenoy, V. Van Doren, P. Geerlings, Ab initio study of the elastic properties of single-walled carbon nanotubes and graphene, Chem. Phys. Lett. 326 (1-2) (2000) 181–185.
[5] J. Hone, Phonons and thermal properties of carbon nanotubes, in: Carbon Nanotubes, Springer, 2001, pp. 273–286.
[6] I.D. Rosca, S.V. Hoa, Highly conductive multiwall carbon nanotube and epoxy composites produced by three-roll milling, Carbon 47 (8) (2009) 1958–1968.
[7] M. Fujii, X. Zhang, H. Xie, H. Ago, K. Takahashi, T. Ikuta, H. Abe, T. Shimizu, Measuring the thermal conductivity of a single carbon nanotube, Phys. Rev. Lett. 95 (6) (2005) 065502.
[8] E. Bekyarova, M.E. Itkis, N. Cabrera, B. Zhao, A. Yu, J. Gao, R.C. Haddon, Electronic properties of single-walled carbon nanotube networks, J. Am. Chem. Soc. 127 (16) (2005) 5990–5995.
[9] J.M. Schnorr, T.M. Swager, Emerging applications of carbon nanotubes, Chem. Mater. 23 (3) (2011) 646–657.
[10] L.A. Girifalco, M. Hodak, R.S. Lee, Carbon nanotubes, buckyballs, ropes, and a universal graphitic potential, Phys. Rev. B. 62 (19) (2000) 13104–13110.
[11] S.B. Sinnott, Chemical functionalization of carbon nanotubes, J. Nanosci. Nanotechnol. 2 (2) (2002) 113–123.
[12] K. Balasubramanian, M. Burghard, Chemically functionalized carbon nanotubes, Small 1 (2) (2005) 180–192.
[13] H. Peng, L.B. Alemany, J.L. Margrave, V.N. Khabashesku, Sidewall carboxylic acid functionalization of single-walled carbon nanotubes, J. Am. Chem. Soc. 125 (49) (2003) 15174–15182.
[14] J. Zhao, H. Park, J. Han, J.P. Lu, Electronic properties of carbon nanotubes with covalent sidewall functionalization, J. Phys. Chem. B 108 (14) (2004) 4227–4230.
[15] E. Chełmecka, K. Pasterny, T. Kupka, L. Stobiński, OH-functionalized open-ended armchair single-wall carbon nanotubes (SWCNT) studied by density functional theory, J. Mol. Model. 18 (4) (2012) 1463–1472.
[16] M. Gao, F. Gao, B. Ma, N. Yu, Z. She, C. Zhao, L. Guo, Y. Zhao, S. Li, C. Jin, Insights into long-term effects of amino-functionalized multi-walled carbon nanotubes (MWCNTs-NH2) on the performance, enzymatic activity and microbial community of sequencing batch reactor, Environ. Pollut. 254 (2019) 113118, https://doi.org/10.1016/j.envpol.2019.113118.
[17] R. Barthos, D. Méhn, A. Demortier, N. Pierard, Y. Morciaux, G. Demortier, A. Fonseca, J.B. Nagy, Functionalization of single-walled carbon nanotubes by using alkyl-halides, Carbon 43 (2) (2005) 321–325.
[18] D. Hines, M.H. Rümmeli, D. Adebimpe, D.L. Akins, High-yield photolytic generation of brominated single-walled carbon nanotubes and their application for gas sensing, Chem. Commun. 50 (78) (2014) 11568–11571.
[19] M. Tavakkoli, M. Nosek, J. Sainio, F. Davodi, T. Kallio, P.M. Joensuu, K. Laasonen, Functionalized carbon nanotubes with Ni (II) bipyridine complexes as efficient catalysts for the alkaline oxygen evolution reaction, ACS Catal. 7 (12) (2017) 8033–8041.
[20] S. Banerjee, S.S. Wong, Functionalization of carbon nanotubes with a metal-containing molecular complex, Nano Lett. 2 (1) (2002) 49–53.
[21] Y. Hwang, S.-H. Park, J.W. Lee, Applications of functionalized carbon nanotubes for the therapy and diagnosis of cancer, Polymers 9 (1) (2017) 13.
[22] Z. Zanolli, R. Leghrib, A. Felten, J.-J. Pireaux, E. Llobet, J.-C. Charlier, Gas sensing with Au-decorated carbon nanotubes, ACS Nano 5 (6) (2011) 4592–4599.
[23] J. Mäklin, T. Mustonen, K. Kordás, S. Saukko, G. Tóth, J. Vähäkangas, Nitric oxide gas sensors with functionalized carbon nanotubes, Phys. Stat. Sol. (b) 244 (11) (2007) 4298–4302.
[24] Y.-J. Xu, A. Rosa, L. Xi, D.-S. Su, Characterization and use of functionalized carbon nanotubes for the adsorption of heavy metal anions, New Carbon Mater. 26 (1) (2011) 57–62.
[25] M.A. Tofighy, T. Mohammadi, Copper ions removal from aqueous solutions using acid-chitosan functionalized carbon nanotubes sheets, Desalin. Water Treat. 57 (33) (2016) 15384–15396.
[26] M. Amosa, I. Mohammed, S. Yaro, Sulphide scavengers in oil and gas industry–a review, Nafta 61 (2) (2010) 85–92.
[27] P. Patnaik, A Comprehensive Guide to the Hazardous Properties of Chemical Substances, John Wiley & Sons, 2007.
[28] T.H.J. Florin, Hydrogen sulphide and total acid-volatile sulphide in faeces, determined with a direct spectrophotometric method, Clin. Chim. Acta 196 (2-3) (1991) 127–134.
[29] M. Colon, J.L. Todolí, M. Hidalgo, M. Iglesias, Development of novel and sensitive methods for the determination of sulfide in aqueous samples by hydrogen sulfide generation-inductively coupled plasma-atomic emission spectroscopy, Anal. Chim. Acta 609 (2) (2008) 160–168.
[30] C. Giuriati, S. Cavalli, A. Gorni, D. Badocco, P. Pastore, Ion chromatographic determination of sulfide and cyanide in real matrices by using pulsed amperometric detection on a silver electrode, J. Chromatogr. A 1023 (1) (2004) 105–112.
[31] D. Giovanelli, N.S. Lawrence, S.J. Wilkins, L. Jiang, T.G. Jones, R.G. Compton, Anodic stripping voltammetry of sulphide at a nickel film: towards the development of a reagentless sensor, Talanta 61 (2) (2003) 211–220.
[32] C.J. Richardson, E.A.M. Magee, J.H. Cummings, A new method for the determination of sulphide in gastrointestinal contents and whole blood by microdistillation and ion chromatography, Clin. Chim. Acta 293 (1-2) (2000) 115–125.
[33] N. Shahbazi, R. Zare-Dorabei, Probe for sensitive direct determination of sulphide ions based on gold nanoparticles, IET Nanobiotechnol. 12 (8) (2018) 1140–1143.
[34] C. Goyenola, G.K. Gueorguiev, S. Stafström, L. Hultman, Fullerene-like CSx: a first-principles study of synthetic growth, Chem. Phys. Lett. 506 (1-3) (2011) 86–91.
[35] C. Goyenola, S. Stafström, L. Hultman, A.G.K. Gueorguiev, Structural patterns arising during synthetic growth of fullerene-like sulfocarbide, J. Phys. Chem. C. 116 (39) (2012) 21124–21131.
[36] Z.D. Lin, S.J. Young, C.H. Hsiao, S.J. Chang, Adsorption sensitivity of Ag-decorated carbon nanotubes toward gas-phase compounds, Sens. Actuators, B 188 (2013) 1230–1234.
[37] M. Frisch, G. Trucks, H. Schlegel, G. Scuseria, M. Robb, J. Cheeseman, G. Scalmani, V. Barone, B. Mennucci, G. Petersson, Gaussian D01, Inc., Wallingford, CT, USA. 2010.
[38] R. Dennington, T. Keith, J. Millam, GaussView, version 5, 2009.
[39] B. Merabet, A.J.H. Almaliky, A.H. Reshak, M.M. Ramli, J. Bila, Dielectric absorption correlated to ferromagnetic behavior in (Cr, Ni)-codoped 4H–SiC for microwave applications, J. Mol. Struct. 1248 (2022) 131462, https://doi.org/10.1016/j.molstruc.2021.131462.
[40] H. Yu, H. Huang, A.H. Reshak, S. Auluck, L. Liu, T. Ma, Y. Zhang, Coupling ferroelectric polarization and anisotropic charge migration for enhanced CO2 photoreduction, Appl. Catal. B 284 (2021) 119709, https://doi.org/10.1016/j.apcatb.2020.119709.
[41] R. Ullah, A.H. Reshak, M.A. Ali, A. Khan, G. Murtaza, M. AL-Anazy, H. Althib, T.H. Flemban, Pressure-dependent elasto-mechanical stability and thermoelectric properties of MYbF3 (M= Rb, Cs) materials for renewable energy, Int. J. Energy Res. 45 (6) (2021) 8711–8723.
[42] S. Tabassam, A.H. Reshak, G. Murtaza, S. Muhammad, A. Laref, M. Yousaf, AM. M. Al Bakri, J. Bila, Co2YZ (Y= Cr, Nb, Ta, V and Z= Al, Ga) Heusler alloys under the effect of pressure and strain, J. Mol. Graph. Model. 104 (2021) 107841, https://doi.org/10.1016/j.jmgm.2021.107841.
[43] R. Singla, S. Kumar, T.A. Hackett, A.H. Reshak, M.K. Kashyap, Genesis of magnetism in graphene/MoS2 van der Waals heterostructures via interface engineering using Cr-adsorption, J. Alloy. Compd. 859 (2021) 157776, https://doi.org/10.1016/j.jallcom.2020.157776.
[44] M. Husain, N. Rahman, A.H. Reshak, Zulfiqar, A. Habib, S. Ali, A. Laref, A.M.M. Al Bakri, J. Bila, Insight into the physical properties of the inter-metallic titanium-based binary compounds, Eur. Phys. J. Plus. 136 (6) (2021), https://doi.org/10.1140/epjp/s13360-021-01590-x.
[45] C. Wang, L. Zhang, Y. Jiang, M. Zhang, L. Liu, D. Ye, S. Zhang, Y.u. Yang, A DFT study on the high-density assembly of doxorubicin drug delivery by single-walled carbon nanotubes, Physica E 134 (2021) 114892, https://doi.org/10.1016/j.physe.2021.114892.
[46] N. Saikia, R.C. Deka, Density functional calculations on adsorption of 2-methylheptylisonicotinate antitubercular drug onto functionalized carbon nanotube, Comput. Theor. Chem. 964 (1) (2011) 257–261, https://doi.org/10.1016/j.comptc.2011.01.006.
[47] M. Yoosefian, A. Pakpour, N. Etminan, Nanofilter platform based on functionalized carbon nanotubes for adsorption and elimination of Acrolein, a toxicant in cigarette smoke, Appl. Surf. Sci. 444 (2018) 598–603, https://doi.org/10.1016/j.apsusc.2018.03.108.
[48] M.S. Dresselhaus, G. Dresselhaus, P.C. Eklund, Science of Fullerenes and Carbon Nanotubes: Their Properties and Applications, Elsevier, 1996.
[49] V.A.E. Barrios, J.R.R. Méndez, N.V.P. Aguilar, G.A. Espinosa, J.L.D. Rodríguez, FTIR–an essential characterization technique for polymeric materials, InTech (2012).
[50] N. Kouklin, M. Tzolov, D. Straus, A. Yin, J. Xu, Infrared absorption properties of carbon nanotubes synthesized by chemical vapor deposition, Appl. Phys. Lett. 85 (19) (2004) 4463–4465.
[51] R. Yudianti, H. Onggo, Y. Saito, T. Iwata, J.-i. Azuma, Analysis of functional group sited on multi-wall carbon nanotube surface, Open Mater. Sci. J. 5 (1) (2011).
[52] C. Ewels, M. Glerup, V. Krstic, V. Basiu, E. Basiuk, Nitrogen and boron doping in carbon nanotubes, Chem. Carbon Nanotubes (2007,) 1–82.
[53] A. Misra, P.K. Tyagi, M.K. Singh, D.S. Misra, FTIR studies of nitrogen doped carbon nanotubes, Diam. Relat. Mater. 15 (2-3) (2006) 385–388.

[54] L.-H. Teng, T.-d. Tang, IR study on surface chemical properties of catalytic grown carbon nanotubes and nanofibers, J. Zhejiang Univ.-Sci. A. 9 (5) (2008) 720–726.
[55] L. Liao, C. Pan, Enhanced electrochemical capacitance of nitrogen-doped carbon nanotubes synthesized from amine flames, Soft Nanosci. Lett. 01 (01) (2011) 16–23.
[56] Z.-M. Dang, L. Wang, L.-P. Zhang, Surface functionalization of multiwalled carbon nanotube with trifluorophenyl, J. Nanomater. 2006 (2006) 1–5.
[57] A.G. Ryabenko, T.V. Dorofeeva, G.I. Zvereva, UV–VIS–NIR spectroscopy study of sensitivity of single-wall carbon nanotubes to chemical processing and Van-der-Waals SWNT/SWNT interaction. Verification of the SWNT content measurements by absorption spectroscopy, Carbon 42 (8-9) (2004) 1523–1535.
[58] H. Kataura, Y. Kumazawa, Y. Maniwa, I. Umezu, S. Suzuki, Y. Ohtsuka, Y. Achiba, Optical properties of single-wall carbon nanotubes, Synth. Met. 103 (1-3) (1999) 2555–2558.
[59] N. Hamada, S.-I. Sawada, A. Oshiyama, New one-dimensional conductors: graphitic microtubules, Phys. Rev. Lett. 68 (10) (1992) 1579–1581.
[60] J.W.G. Wilder, L.C. Venema, A.G. Rinzler, R.E. Smalley, C. Dekker, Electronic structure of atomically resolved carbon nanotubes, Nature 391 (6662) (1998) 59–62.
[61] S. Hussain, P. Jha, A. Chouksey, R. Raman, S.S. Islam, T. Islam, P.K. Choudhary, Spectroscopic investigation of modified single wall carbon nanotube (SWCNT), J. Modern Phys. 02 (06) (2011) 538–543.
[62] Y. Li, S. Kodama, T. Kaneko, R. Hatakeyama, Performance enhancement of solar cells based on single-walled carbon nanotubes by Au nanoparticles, Appl. Phys. Lett. 101 (8) (2012) 083901, https://doi.org/10.1063/1.4739427.
[63] G. Bereket, E. Hür, C. Öğretir, Quantum chemical studies on some imidazole derivatives as corrosion inhibitors for iron in acidic medium, J. Mol. Struct. (Thoechem) 578 (1-3) (2002) 79–88.
[64] N. Saikia, R.C. Deka, Density functional calculations on adsorption of 2-methylheptylisonicotinate antitubercular drug onto functionalized carbon nanotube, Comput. Theoretical Chem. 964 (1-3) (2011) 257–261.
[65] P.A. Cox, Ionization energies of open-shell molecules in the frozen orbital approximation, Mol. Phys. 30 (2) (1975) 389–403.
[66] T. Tsuneda, J.-W. Song, S. Suzuki, K. Hirao, On Koopmans' theorem in density functional theory, J. Chem. Phys. 133 (17) (2010) 174101, https://doi.org/10.1063/1.3491272.